Gas Transport Properties of Polyaniline Membranes

MIN-JONG CHANG, YUN-HSIN LIAO, ALLAN S. MYERSON, and T. K. KWEI*

Department of Chemical Engineering, Polytechnic University, 6 Metrotech Center, Brooklyn, New York 11201

SYNOPSIS

The transport properties of He, H_2, CO_2, O_2, N_2, and CH_4 gases in solvent cast, HCl doped, and undoped polyaniline (PANi) membranes were determined. Measurements were carried out at 40 psi pressure from 19°C to 60°C. An excellent correlation was found between the diffusion coefficients and the molecular diameters of gases. The solubility coefficients of gases were found to correlate with their boiling points or critical temperatures. The separation factors for CO_2/N_2 and CO_2/CH_4 are dominated by the high solubility of CO_2. These correlations enable us to predict the permeability, diffusion, and solubility coefficients of other gases. After the doping–undoping process, the fluxes of gases with kinetic diameters smaller than 3.5 Å increased but those of larger gases decreased. This results in a higher separation factor for a gas pair involving a small gas molecule and a larger one. © 1996 John Wiley & Sons, Inc.

INTRODUCTION

Gas separation by polymer membranes has been the subject of intense research activities.[1] Polyaniline (PANi) has attracted attention recently because it has been reported to have very high gas separation efficiencies.[2-4] Of particular interest was the observation that the morphologies of PANi membranes can be tailored after film formation through doping–undoping processes.[5,6] The nature of the dopant and its concentration was found to affect gas permeability of the membrane and its separation efficiency.[7,8]

In many previous publications, only the permeation coefficients were reported. In order to acquire a better understanding of the structure factors which influence gas permeation, it is necessary to resolve the permeation coefficient into its two components, namely, the diffusion coefficient and the solubility coefficient. In this paper we report the results of such an investigation. The dependence of diffusion and solubility coefficients on the properties of the gases and the polymers were analyzed. We also found that the undoping process increased the permeabilities of gases having kinetic diameters smaller than about 3.5 Å but decreased the permeabilities for gases having larger sizes.

EXPERIMENTAL

Materials

PANi was prepared by the oxidative polymerization of aniline[9] (Aldrich Chemical Co., USA). Aniline (0.4 mol) was dissolved in 500 mL 1*N* HCl, and the oxidant, ammonium persulfate (Aldrich Chemical Co., 0.1 mol), was dissolved separately in 500 mL 1*N* HCl. Both solutions were cooled in an ice bath. The oxidant solution was poured into the monomer solution with constant stirring. The reaction mixture was kept in the ice bath for 1 h, and then was brought to room temperature and allowed to react for another 3 h.

The PANi hydrochloride salt was subsequently isolated from the reaction mixture by filtration. The powder was washed with an excess of 1*N* HCl to remove the oxidant and oligomers. The hydrochloride salt was subsequently neutralized in 0.1*N* ammonium hydroxide for 12 h to obtain the base form (structure a in Fig. 1). The PANi base was washed with excess ammonium hydroxide and with water, and rinsed with diethyl ether. The powder was dried in a vacuum oven at 50°C for 12 h under nitrogen atmosphere.

* To whom correspondence should be addressed.

Journal of Applied Polymer Science, Vol. 62, 1427–1436 (1996)
 CCC 0021-8995/96/091427-10

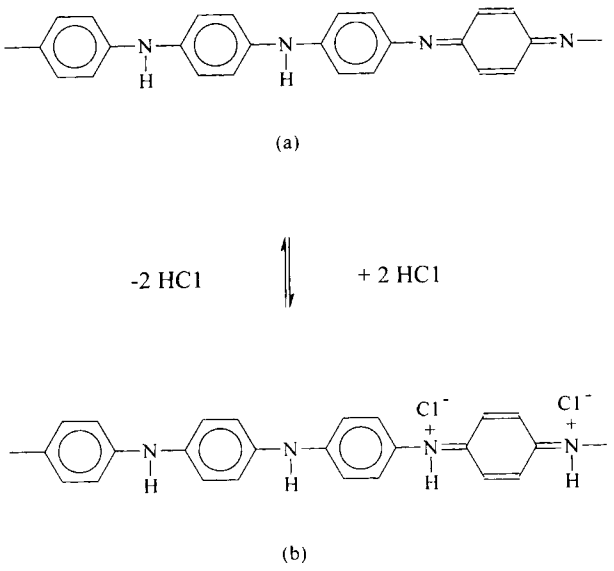

Figure 1 Polyaniline in (a) the base and (b) the HCl-doped forms.

N-methyl-2-pyrrolidone (NMP) (Aldrich Chemical Co.) solutions of PANi were prepared by adding the polymer slowly to NMP with constant stirring for 12 h, followed by filtration through 0.45-μm syringe filters. The resultant solutions were placed in petri dishes and dried for 24 h at 120°C in a vacuum oven. Freestanding, flexible, and copper-colored films could be peeled off from the glass substrates. Doping was carried out by immersing the emeraldine base film in 1*M* aqueous HCl to yield flexible, lustrous blue films of emeraldine hydrochloride[10] (structure b in Fig. 1). The samples were undoped by treating with 1*N* NH_4OH solution for at least 48 h to remove the halogen ions from the films.[2] Before gas permeation experiments were performed, the membranes were immersed in deionized water for 2 days and then dried for 24 h at room temperature in a vacuum oven. This step was important to minimize the amount of residual casting solvent in the films in order to obtain reproducible results. The membranes are about 100 μm in thickness.

Characterization

Thin films of PANi for ultraviolet (UV) and infrared (IR) measurement were prepared by spinning a 5% NMP solution on quartz and NaCl crystal windows. The UV/Visible/near IR spectra were recorded on a Perkin-Elmer Lambda 9 Spectrometer. The IR spectra were measured by the use of a Nicolet 710 FT-IR Spectrometer.

A thermogravimetric analyzer (TGA, Du-Pond Model 951) was used to measure weight losses of PANi powder, PANi membrane containing residual NMP, and HCl-doped PANi film. Spectra were scanned from 25 to 600°C with a heating rate of 10°C/min under a nitrogen stream.

Wide-angle x-ray diffractometry (Philips Model APD-3720) was used to examine chain packing in the as-cast PANi film and HCl-doped PANi powder. The samples were scanned from 2 to 60° (2θ) at a rate of 0.01°/s.

Measurement of Gas Permeability

Gas permeability coefficients were determined by using the high-vacuum method.[11] After both sides of a membrane were evacuated, the permeant was introduced to the upstream side of the membrane at 40 psi, and was allowed to permeate to the downstream side (0.02 Torr). After a certain period of time, a steady state was reached at which the amount of gas permeated increased linearly with time. The permeability coefficient was calculated from the slope of the straight line. These measurements were carried out at 19 to 60°C for He, H_2, CO_2, O_2, N_2, and CH_4.

Because permeation is a solution–diffusion process, the individual contributions to the permeability, P, by the diffusion and solubility coefficients can be expressed by the following equation:

$$P = DS \tag{1}$$

where D, the diffusion coefficient, represents the penetrant mobility as it moves from the upstream to the downstream face of the membrane; and S, the effective solubility coefficient, is thermodynamic in nature and is influenced by the condensibility of the penetrant, polymer–penetrant interactions, and the amount of excess interchain gaps existing in a glassy polymer.[12]

In order to measure P and S by a single experiment, the "time lag" method was used in which P was obtained from the steady-state portion of the permeation curve and D was calculated from the time lag, θ, given by the relationship[13]:

$$D = L^2/6\theta \tag{2}$$

where L is the thickness of the film. The solubility is then calculated using eq. (1) as the ratio of P to D.

When the downstream pressure is negligible relative to the upstream pressure, the separation factor

of a membrane for a gaseous mixture of A and B can be related simply to the permeabilities of A and B in terms of the mobility and solubility terms, *viz.*,

$$\alpha^*_{AB} = \frac{P_A}{P_B} = \frac{[D_A]}{[D_B]} \times \frac{[S_A]}{[S_B]} = \alpha_D \times \alpha_S \qquad (3)$$

where α^*_{AB} is called the "ideal separation factor," and α_D and α_S are the "diffusion selectivity" and "solubility selectivity," respectively. The ideal mixture selectivity can be approximated by using the pure-component permeabilities up to the point at which "plasticization" of the polymer by the gas is said to occur,[14] for example, in the case of CO_2 diffusion in polycarbonate at high pressures.[15] Our experiments were carried out at sufficiently low pressures that the plasticization effect was believed to be absent.

The apparent activation energies of permeation (E_P), diffusion (E_D), and the enthalpy of solution (ΔH_S) were calculated from the temperature coefficients of P, D, and S, respectively. These quantities are related by eq. (4):

$$\Delta H_S = E_P - E_D \qquad (4)$$

The experimental errors vary with the magnitudes of the permeability and time lag. The estimated errors in gas permeability, diffusion, and solubility coefficients are about 5 to 15% for He, H_2, CO_2, and O_2, and about 20 to 30% for N_2 and CH_4. The errors in E_P, E_D, and ΔH_S are estimated to be about 10% for He, H_2, CO_2, and O_2, and about 20% for N_2.

RESULTS AND DISCUSSION

Characterizations of PANi and HCl-doped PANi

The UV/Visible absorption spectra of PANi and HCl-doped PANi are shown in Figure 2. The absorption spectrum of PANi shows two maxima: the one at 323 nm is assigned to the π to π^* transition of a benzenoid amine structure; and the other, at 603 nm, is due to a quinoid structure.[16-19] When PANi is doped by HCl, the peak at 603 nm is transformed to a free carrier tail which indicates the polaron band, due to the delocalization of radical cation,[20] extending to near the IR range.

The IR spectra of PANi are shown in Figure 3. The N—H stretching band of PANi is located at 3290 cm^{-1} and the aromatic C—H stretching band at 3050 cm^{-1}. The 1595 cm^{-1} and 1500 cm^{-1} absorptions are assigned to vibrations of the quinoid and benzenoid rings of PANi, respectively. The C—N—C stretching appears at 1303 cm^{-1}, and the bands at 1167 and 831 cm^{-1} are attributed to the aromatic C—H in plane and out-of-plane bending, respectively.

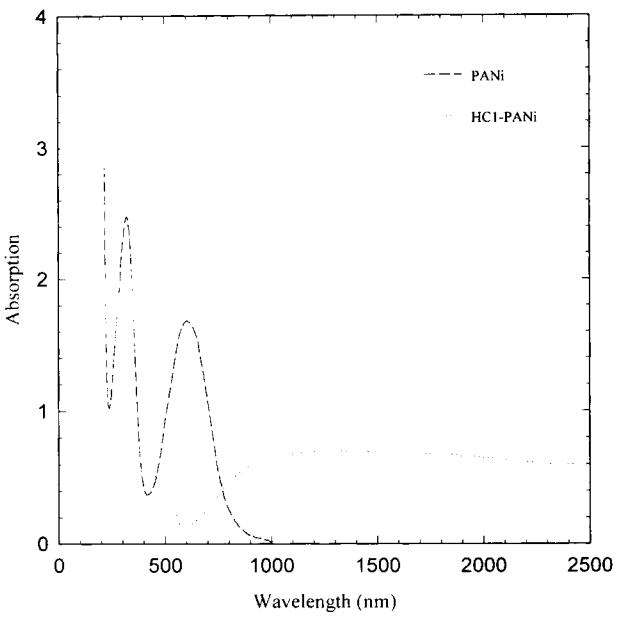

Figure 2 The UV-vis spectra of the base and HCl-doped PANi.

Figure 4 shows the results of TGA measurements of PANi powder, NMP plasticized PANi film, and HCl-doped PANi film. The PANi powder decomposes at about 470°C. For the PANi film the weight loss begins at about 100°C and reaches about 10% at 300°C; the loss in weight in this temperature range is primarily due to removal of the residual NMP. Similarly, the weight loss of HCl-doped PANi is also about 10% at 300°C due to the evaporation of NMP. The films start to decompose at temperatures above 300°C.

X-ray diffraction patterns of PANi powder, HCl-doped PANi powder, and undoped PANi film are shown in Figure 5. The PANi powder exhibits a broad amorphous peak at about 4.6 Å ($2\theta \cong 19°$) and a weak peak at about 24°. The undoped PANi film, which may still contain a small amount of NMP, shows only one amorphous peak at about 4.6 Å; however, HCl-doped PANi powder shows a clear diffraction peak with d spacing of 3.5 Å, indicating that the interchain alignment becomes more ordered. Our result is similar to the report of Chen and Lee.[21] The dominant d spacing corresponds roughly to intermolecular chain spacing.[15]

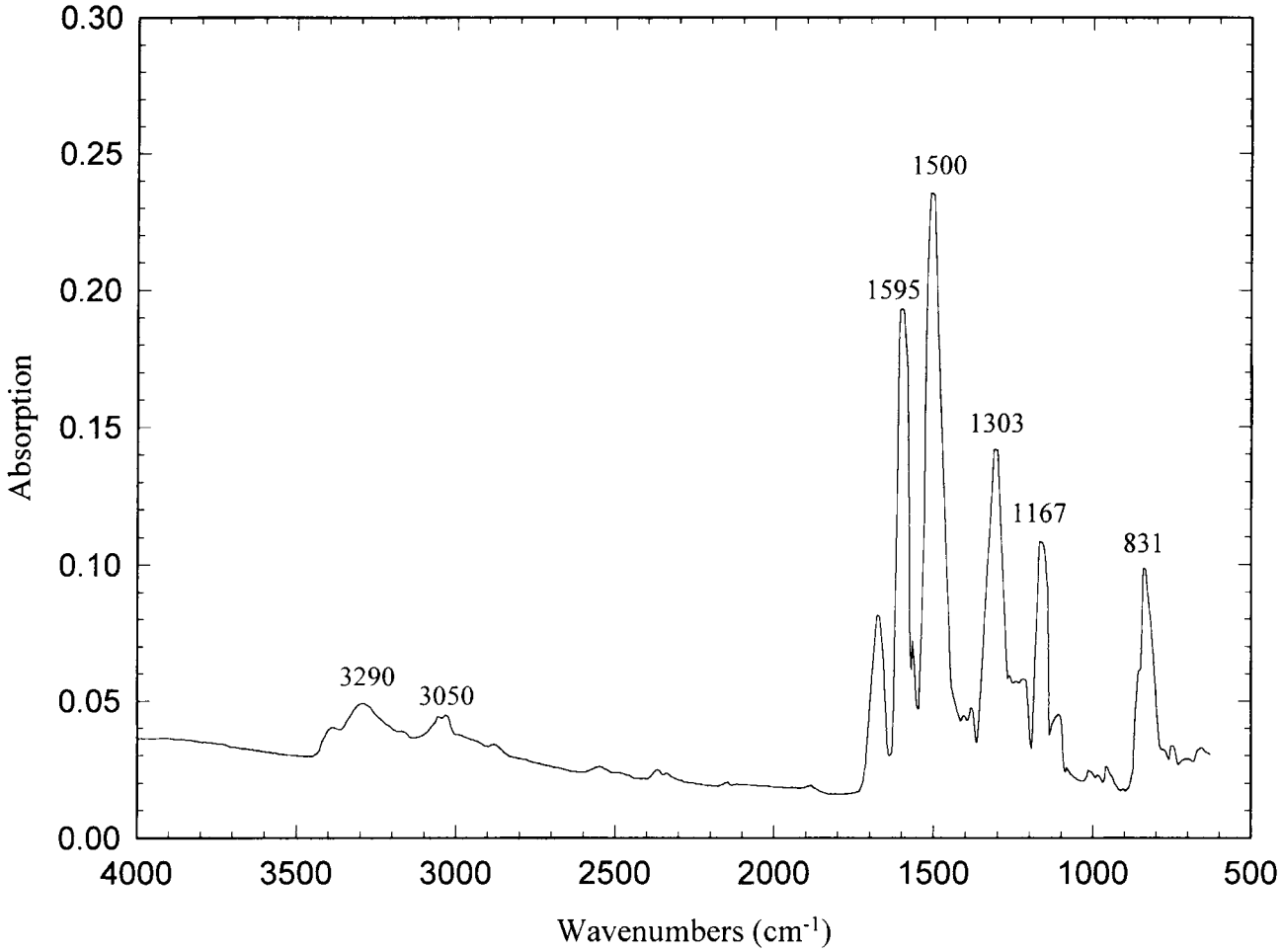

Figure 3 The IR spectra of PANi.

Gas Transport Properties in PANi Membrane—General Features

In Figures 6 and 7, the permeability and apparent diffusion coefficients for the six gases (He, H_2, CO_2, O_2, N_2, and CH_4) in the as-cast PANi membrane are shown as a function of temperature. Except for CH_4, for which there was insufficient data, linear relationships were obtained from the Arrhenius plots of permeability coefficients. The apparent diffusion coefficient of He could not be determined accurately in our experiment because its time lag was too small. However, plots of ln D against the reciprocal temperature for H_2, CO_2, O_2, and N_2 were linear. The solubility coefficients of these gases, which are the ratios of permeability coefficients to the respective diffusion coefficients, are listed in Table I.

At each temperature, the permeability, diffusion, and solubility coefficients were ranked as follows:

$$P_{He} > P_{H_2} > P_{CO_2} > P_{O_2} > P_{N_2} > P_{CH_4}$$

$$D_{He} > D_{H_2} > D_{O_2} > D_{CO_2} > D_{N_2} > D_{CH_4}$$

$$S_{CO_2} > S_{CH_4} > S_{O_2} \cong S_{N_2} > S_{H_2}$$

The order of diffusion coefficients for these gases is the same as that of permeability coefficients, except for CO_2, due to its highest solubility. The same trend was also found by Rebattet and colleagues.[22] Additionally, the order of E_P (Table II) is the reverse of that of permeability coefficients; that is, high activation energies are associated with lower permeability coefficients in the temperature range of our experiments. The same relationship holds for E_D and diffusion coefficients except for N_2, possibly due to the less accurate value in E_D for N_2. The enthalpy of solution is primarily dependent on gas condensibility.

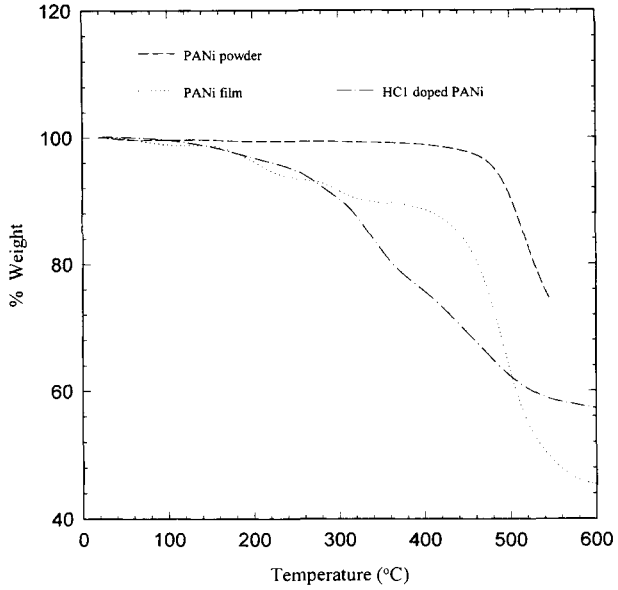

Figure 4 TGA curves of PANi powder, NMP-plasticized PANi, and HCl-doped PANi films.

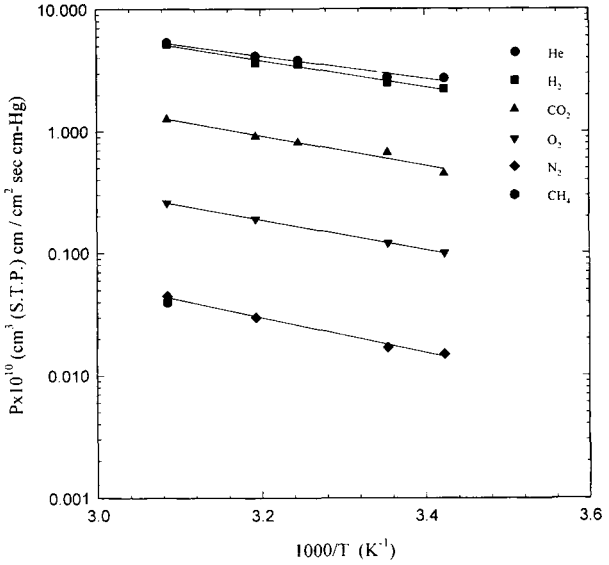

Figure 6 Permeability coefficients of selected gases as a function of reciprocal absolute temperature for PANi membrane.

In order to examine the effect of gas solubility on permeability more clearly, the ideal separation factor, the diffusion selectivity and solubility selectivity were calculated and are listed in Table III. By comparing α_D and α_S for selected gas pairs, it can be seen that the difference in gas solubilities dominates the separation efficiency for the CO_2/N_2 and CO_2/CH_4 pairs due to high CO_2 solubility. On the other hand, the separation factors are primarily controlled by the differences in diffusion coefficients for the other gas pairs. Similar phenomena were found for gas permeation in the poly(chloro-*p*-xylylene) membrane.[23]

Many investigators reported correlations[2] between the kinetic diameters of gases and their permeabilities in polymers. Although such a correlation also appears to be applicable to our results (Fig. 8),

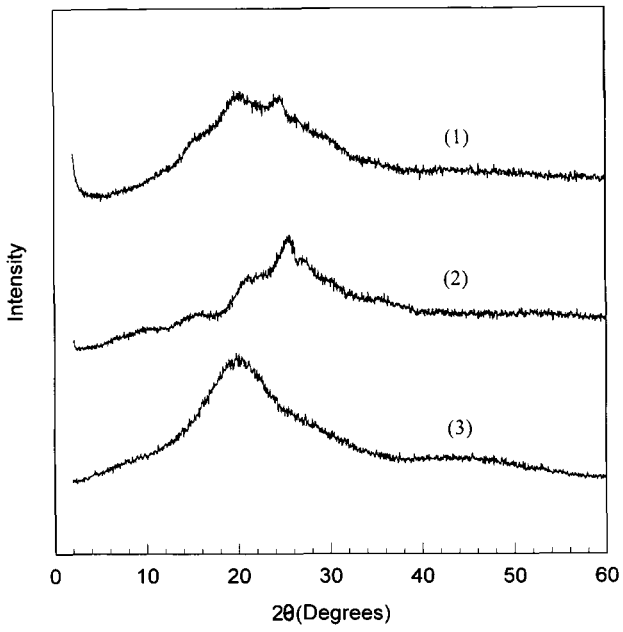

Figure 5 X-ray diffraction patterns of the (1) PANi powder, (2) HCl-doped PANi powder, and (3) undoped PANi film.

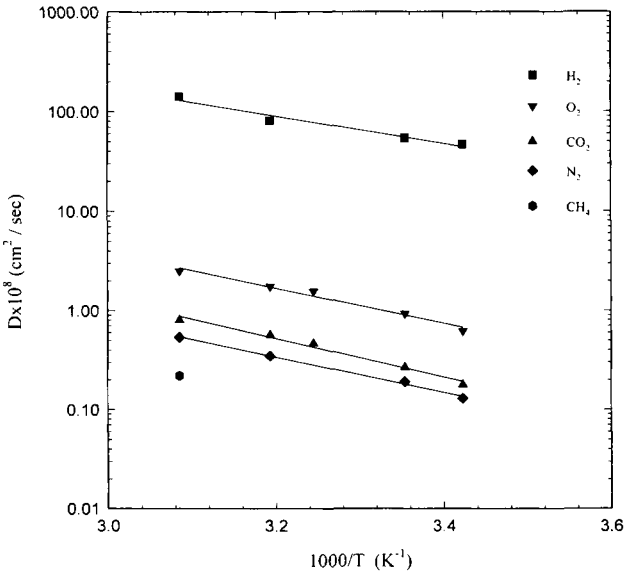

Figure 7 Temperature dependence of diffusion coefficients for selected gases in the PANi membrane.

Table I Temperature Dependence of Solubility Coefficients for Selected Gases in the PANi Membrane

Gas	19°C	25°C	35°C	40°C	51°C
H_2	0.477	0.463	—	0.451	0.367
CO_2	25.1	24.90	17.3	15.9	15.7
O_2	1.61	1.29	—	1.07	1.04
N_2	1.154	0.890	—	0.857	0.83
CH_4	—	—	—	—	1.82

Unit of solubility coefficient: 10^{-3} cm^3 (STP)/cm^3 cm Hg.

the correlation masks the important contribution of solubility to permeability. In the following, the diffusion and solubility coefficients are discussed separately in order to clarify the influence of the molecular parameters.

Correlation for Solubility Coefficients

The gas solubility in a given polymer generally follows the tendency of the gas to form a condensed phase. Therefore, it is expected that gas sorption would decrease in the order: $CO_2 > CH_4 > O_2 > N_2$. Linear relationships have been found by Van Amerongen[24] between the solubility coefficients of various gases in natural rubber and the boiling points of the gases, or their critical temperatures. The results can be described by the following expressions:

$$\ln S = 0.028T_b - 9.15 \quad \text{at } 25°C \tag{5}$$

$$\ln S = 0.017T_c - 9.15 \quad \text{at } 25°C \tag{6}$$

where S is the gas solubility in [cm^3 (STP)]/cm^3 cm Hg) and T_b and T_c are the boiling points and critical temperatures of the gases in °K, respectively. Plots illustrating similar correlations for CO_2, O_2, N_2, and CH_4 in the PANi film are shown in Figure 9, and the correlation eqs. (7) and (8) are nearly identical with Van Amerongen's findings.

$$\ln S = 0.026T_b - 9.12 \quad \text{at } 51°C \tag{7}$$

$$\ln S = 0.017T_c - 9.42 \quad \text{at } 51°C \tag{8}$$

From the two relationships, we estimate the He solubility coefficient in PANi to be about 1.05×10^{-4} [cm^3 (STP)]/cm^3 cm Hg). The diffusion coefficient of He is then calculated from eq. (1) to be about 5×10^{-6} (cm^2/s), which is at the limit of the accuracy of our time-lag measurements for the film thickness used.

Correlation for Diffusion Coefficients

Michaels and Bixler[25] found a relationship between reduced diffusion constant and the reduced molecular diameter for amorphous polyethylene:

$$\ln(D/d^2) = A[d - (\phi^{1/2}/2)] + b \tag{9}$$

where A and b are temperature dependent constants, and $\phi^{1/2}/2$ is a dimension associated with the free volume per unit length of the chain and is a characteristic of the polymer. The quantity d is the molecular diameter of the gas, which is estimated from eq. (10) by taking into account the possibility of the orientation of the asymmetric molecules during the diffusion jump,

$$d = d_g^2/d_l \tag{10}$$

where d_g and d_l are molecular size parameters summarized in Table IV.[25]

Because $\phi^{1/2}$ is a characteristic of the polymer, a logarithmic plot of reduced diffusion constant (D/d^2) versus d should be linear with a slope of A. This is indeed the case, as shown in Figure 10. From the linear relation at 51°C, we determine the value of

Table II Apparent Activation Energies of Permeation, Diffusion, and Enthalpy of Solution for Selected Gases in PANi Membranes

Membrane	Gas	E_P (kJ/mol)	E_D (kJ/mol)	ΔH_S (kJ/mol)
PANi	He	17.5	—	—
	H_2	20.8	26.4	−5.60
	CO_2	23.5	37.3	−13.8
	O_2	23.8	34.2	−10.4
	N_2	27.6	34.2	−6.60
HCl–PANi	He	40.3	—	—
	H_2	54.0	58.7	−4.71

Table III Temperature Dependence of Ideal Separation Factor (α_P), Diffusion Selectivity (α_D), and Solubility Selectivity (α_S) for Selected Gas Pairs in PANi Membrane

Gas Pair	19°C	25°C	40°C	51°C
Separation Factor				
He/N_2	182	164	138	119
H_2/N_2	149	148	122	116
CO_2/N_2	30.0	39.4	30.3	28.2
O_2/N_2	6.67	7.06	6.33	5.78
CO_2/CH_4	—	134	—	31.8
Diffusion Selectivity				
H_2/N_2	362	284	232	263
CO_2/N_2	1.38	1.41	1.63	1.49
O_2/N_2	4.78	4.85	5.06	4.65
CO_2/CH_4	—	—	—	3.67
Solubility Selectivity				
H_2/N_2	0.413	0.520	0.526	0.442
CO_2/N_2	21.8	28.0	18.6	18.9
O_2/N_2	1.40	1.45	1.25	1.25
CO_2/CH_4	—	—	—	8.63

A from the slope to be −4.9 and that of $(b - A\phi^{1/2}/2)$ from the intercept to be 34.1.

Relationship between E_D and Gas Diameter

It was well established in the literature that there existed a linear relation between ln D and E_D.[26] If $\ln(D/d^2)$ can be correlated with d, E_D should be similarly correlated. According to the activated zone theory,[27] E_D can be expressed as the sum of an intermolecular term, E_i, and an intramolecular term, E_b. If E_i is predominant, E_D will vary directly with the penetrant molecular diameter. On the other hand, E_D will vary with the square of the penetrant molecular diameter, if E_b is predominant.[11] The linear relation between the molecular diameters of the gases and their E_Ds is shown in Figure 11. The results suggest that the major contributor to E_D is the intermolecular force which needs to be overcome in order to create "holes" of sufficient size for the pen-

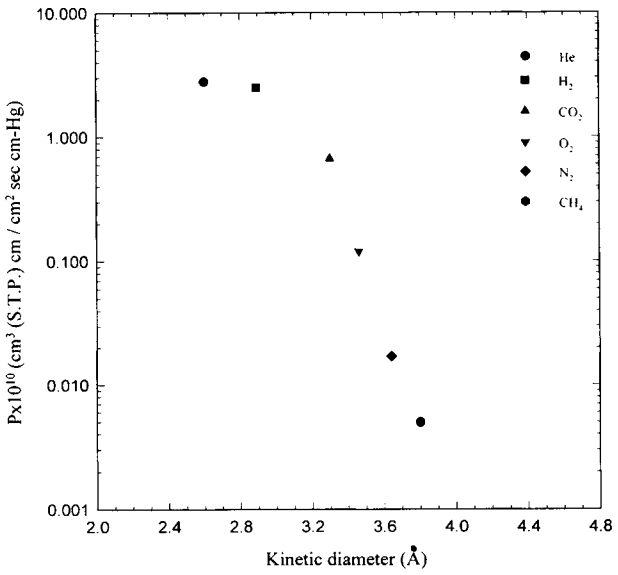

Figure 8 Relation between the kinetic diameters of selected gases and their permeability through the PANi at 25°C.

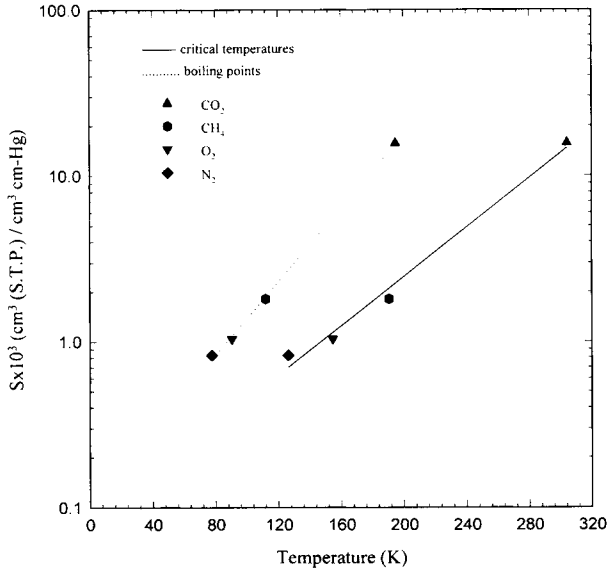

Figure 9 Solubility coefficients of selected bases versus their critical temperatures and boiling points for PANi at 51°C.

Table IV Molecular Size Parameters for Selected Gases

Gas	d_g, Å[a]	d_l, Å[b]	d, Å[c]	Kinetic Diameter, Å
He	2.2		2.2	2.60
H_2	2.7		2.7	2.89
CO_2	4.3	4.8	3.9	3.30
O_2	3.5		3.5	3.46
N_2	3.7		3.7	3.64
CH_4	4.1		4.1	3.80

[a] Gas diameter (from viscosity measurement).
[b] Maximum dimension of molecule from Sturat model.
[c] $d = d_g^2/d_l$.

etrant molecule to undergo the jump process, whereas the E_b term has only a minor effect on the resultant diffusion properties.[27] The rigidity of the PANi chain mostly likely inhibits its bending and renders the intramolecular energy term less important.

Gas Transport Properties in HCl-doped PANi Membrane

Because the permeabilities of CO_2, O_2, N_2, and CH_4 in HCl-doped PANi are less than 0.05 Barrer at 25°C, the effect of doping on gas permeation and diffusion as a function of temperature was studied only for He and H_2, and the results are shown in Figures 12 and 13, respectively. The permeability

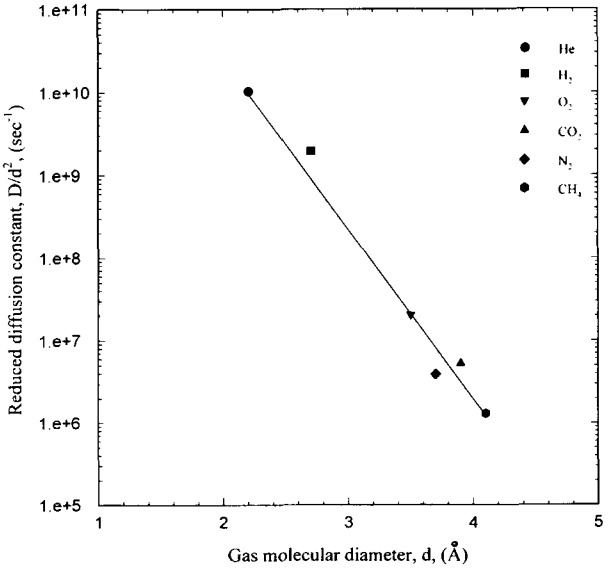

Figure 10 Correlation of the reduced diffusion constants with the molecular diameters for selected gases in PANi at 51°C.

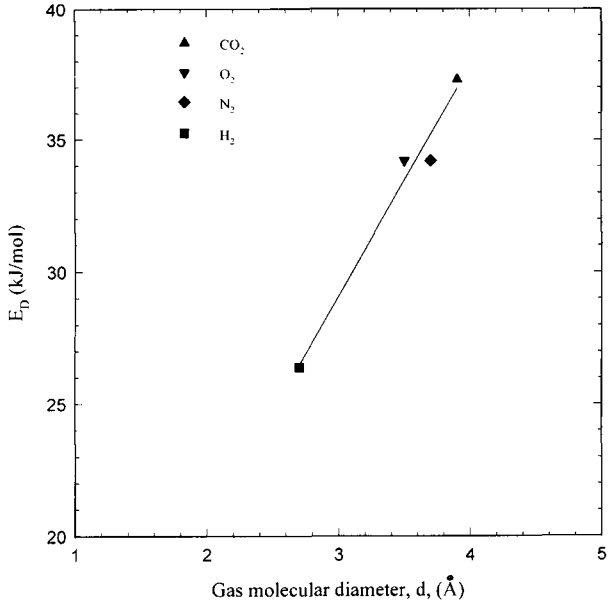

Figure 11 Relation between the molecular diameters of selected gases and their apparent activation energies of diffusion in PANi.

coefficient of He in PANi at 25°C was 2.78 Barrer, but decreased to 0.32 Barrer in HCl-doped PANi. The permeability of H_2 also experienced a decrease from 2.51 to 0.12 Barrers. However, the separation factor, $\alpha_{(He/H_2)}$, increased from 1.11 to 2.67. Interestingly, the solubility of H_2 (Table V) is not significantly altered by doping. Therefore, the doping process causes primarily a decrease in diffusivity.

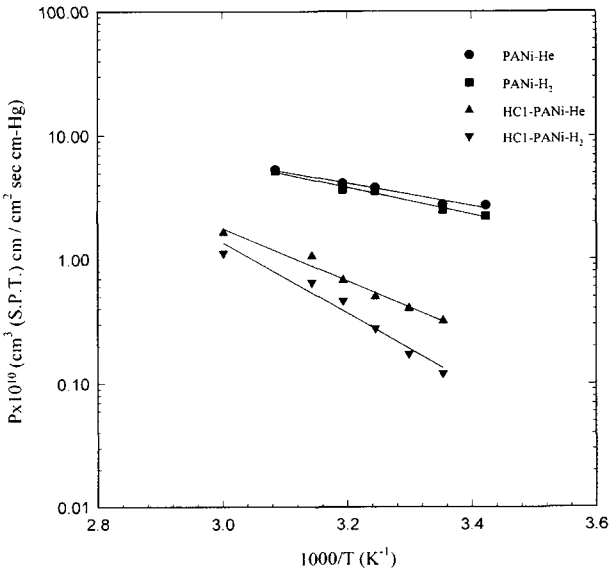

Figure 12 Permeability coefficients of He and H_2 in PANi and HCl-doped PANi.

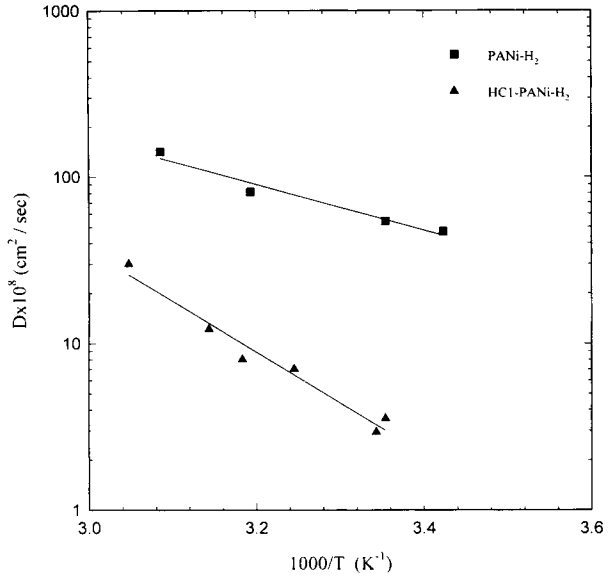

Figure 13 Temperature dependence of diffusion coefficients for H_2 in the PANi and HCl-doped PANi membranes.

Furthermore, the activation energy of diffusion of H_2 is also higher in the doped PANi, 58.4 kJ/mol compared to 26.4 kJ/mol for the base film (Table III).

A possible reason for the decreases in D values of He and H_2 in doped PANi is that the free volume per unit length, represented by $\phi^{1/2}/2$ in eq. (9), has been reduced by the doping process, or that the interchain forces have been increased by the presence of the chloride ions [Fig. 1(b)]. The change in free volume is verified by X-ray spectra which show a decrease in average d spacing from 4.6 Å for PANi to 3.5 Å for HCl-doped PANi. The higher E_D values are then a natural outcome of the additional energy required for hole formation in the diffusional jump process.

Gas Transport Properties in Undoped PANi Membrane

The variations in gas permeabilities of PANi after the doping and undoping processes are listed in Table VI. All gas fluxes decreased with HCl doping due to the presence of the chloride ions which reduce the effective free volume and/or increase interchain forces. However, the undoping treatment produced different results. First, it increased permeabilities by an order of magnitude or more from the values for the HCl-doped film. Second, when compared with the values for the as-cast PANi film, the permeabilities of He, H_2, and CO_2 appear to have increased slightly, but the values for N_2 and CH_4 evidently decreased. Similar results have been reported in the literature.[2,3,22] In grouping the gases according to their kinetic diameters, we find a dividing line at 3.4–3.5 Å. Gases with diameters smaller than 3.4–3.5 Å show increased permeability values after undoping, whereas larger gases show decreased permeabilities. It has been suggested that the distribution of the free volumes in as-cast PANi was shifted toward smaller sizes after doping and undoping treatments.[21]

Table V Temperature Dependence of Solubility Coefficients for Hydrogen in the HCl-doped PANi Membrane

Gas	25°C	35°C	40°C	45°C
H_2	0.3048	0.397	0.577	0.485

Unit of solubility coefficient: 10^{-3} cm^3 (STP)/cm^3 cm Hg.

Comparison of Gas Selectivities with Literature

The ideal separation factors of undoped PANi for the selected gas pairs (Table VII) approximately double the values of as-cast PANi because the doping–undoping process enhances the permeability of smaller gases (He, H_2, CO_2) having kinetic diameters less than 3.5 Å but reduce the permeability of larger gases (N_2, CH_4). Also listed in the table are the data reported by Rebattet and coworkers[22] and Kaner and colleagues[2,3]; our results are comparable to those of Rebattet, but we were unable to reproduce the high separation factors of undoped PANi reported by Kaner.

CONCLUSIONS

Gas solubility selectivities, α_S, are the major contributors to the separation factors for the CO_2/N_2

Table VI Gas Permeabilities of Selected Gases through PANi Membranes at 25°C

	Permeability (Barrer)		
Gas	As-cast	HCl-doped	Undoped
He	2.78	0.319	3.66
H_2	2.51	0.121	3.14
CO_2	0.67	0.034	0.771
O_2	0.12	0.016	0.135
N_2	0.017	< 0.005	0.01
CH_4	0.005	< 0.005	—

Table VII Comparison of Gas Permeability (Barrer) and Selectivity Data with Literature Values

Gas or Gas Pair	Kaner[2,3]	Rebattet[22]	Present Study
	Undoped Film		
He	11.5	—	3.66
H_2	10.6	4.53	3.14
CO_2	1.59	0.568	0.771
O_2	0.172	0.15	0.135
N_2	0.00323	0.016	0.01
CH_4	0.608	0.011	—
	Separation Factors α_P (Undoped Film)		
He/N_2	3560	—	366
H_2/N_2	3280	283	314
O_2/N_2	53	9.4	13.5
CH_4/N_2	188	0.7	—

and CO_2/CH_4 pairs in PANi due to high CO_2 solubility. On the other hand, the differences in diffusion coefficients for the other gas pairs dominate the separation efficiency.

The correlations between the solubility coefficients in PANi and the boiling points of the gases, or their critical temperatures, are nearly identical with that found for natural rubber.

Linear relations were found between the logarithmic reduced diffusion constant and gas diameter, and between activation energy of diffusion and gas diameter. The higher E_D value indicates more energy required to form holes of sufficient size for the diffusion of a larger gas.

As a result of doping, the interchain distance in PANi has been reduced and the interchain forces may be increased by the presence of chloride ions. Therefore, D decreases and E_D increases in doped PANi. Additionally, the solubility of H_2 in PANi is not significantly altered by doping.

The undoping process increased the permeabilities of gases having kinetic diameters smaller than 3.5 Å but decreased the permeability values for larger gases.

REFERENCES

1. W. J. Koros and G. K. Fleming, *J. Membr. Sci.*, **83,** 1 (1993).
2. M. R. Anderson, B. R. Mattes, H. Reiss, and R. B. Kaner, *Science,* **252,** 1412 (1991).
3. J. A. Conklin, S.-C. Huang, and R. B. Kaner, *Polym. Chem.*, **35,** 251 (1994) (Abstr.).
4. M. R. Anderson, B. R. Mattes, H. Reiss, and R. B. Kaner, *Synth. Met.*, **41–43,** 1151 (1991).
5. M. Wan, *J. Polym. Sci., Polym. Chem. Ed.*, **30,** 543 (1992).
6. J. C. Chiang and A. G. MacDiarmid, *Synth. Met.*, **13,** 193 (1986).
7. J. A. Conklin, M. R. Anderson, H. Reiss, and R. B. Kaner, *Polym. Mat. Sci. Eng.*, **72,** 313 (1995) (Abstr.).
8. J. Yang, Q. Sun, X. Hou, and M. Wan, *Chinese Journal of Polymer Science,* **11,** 121 (1993).
9. A. G. MacDiarmid, J. C. Chiang, A. F. Richter, N. L. D. Somasiri, and A. J. Epstein, in *Conducting Polymer,* L. Alcacer, Ed., Reidel Publications, Holland, 1987, p. 105.
10. M. Angelopoulos, A. Ray, and A. G. MacDiarmid, *Synth. Met.*, **21,** 21 (1987).
11. V. Stannett, in *Diffusion in Polymers,* J. Crank and G. S. Park, Eds., Academic Press, London, 1986, Chap. 2.
12. W. J. Koros, *J. Polym. Sci., Polym. Phys. Ed.*, **23,** 1611 (1985).
13. R. M. Barrer, *Trans. Farady Soc.*, **35,** 628 (1939).
14. W. J. Koros and M. W. Hellums, *Fluid Phase Equilibria,* **53,** 339 (1989).
15. M. Aguilar-Vega and D. R. Paul, *J. Polym. Sci., Polym. Phys. Ed.*, **31,** 1599 (1993).
16. Y. Cao, P. Smith, and A. J. Heeger, *Synth. Met.*, **32,** 263 (1989).
17. J. G. Master, Y. Sun, A. G. MacDiarmid, and A. J. Epstein, *Synth. Met.*, **41–43,** 715 (1991).
18. A. P. Monkman, *Mol. Cryst., Liq. Cryst.*, **218,** 253 (1992).
19. S. Srinivasan and P. Pramanik, *Synth. Met.*, **63,** 199 (1994).
20. A. G. MacDiarmid and A. J. Epstein, *Synth. Met.*, **65,** 103 (1994).
21. S. A. Chen and H. T. Lee, *Macromolecules,* **26,** 3254 (1993).
22. L. Rebattet, M. Escoubes, E. Genies, and M. Pineri, *J. Appl. Polym. Sci.*, **57,** 1595 (1995).
23. A. Tanioka, N. Fukushima, K. Hasegawa, K. Miyasaka, and N. Takahashi, *J. Appl. Polym. Sci.*, **54,** 219 (1994).
24. G. J. Van Amerongen, *Rubb. Chem. Technol.*, **37,** 1065 (1964).
25. A. S. Michaels and H. J. Bixler, *J. Polym. Sci.*, **50,** 413 (1961).
26. R. M. Barrer and G. Skirrow, *J. Polym. Sci.*, **3,** 549 (1948).
27. W. W. Brandt, *J. Phys. Chem.*, **63,** 1080 (1959).

Received October 26, 1995
Accepted March 18, 1996